CENTRE FOR RESEARCH IN EXPERIMENTAL SPACE SCIENCE

YORK UNIVERSITY

4700 Keele St, North York, Ontario M3J 1P3

Study of the Shock Combustion of Aromatic and Napthenic Hydrocarbons in Jet Fuels derived from the Canadian Oil Sands

FINAL REPORT

BY

H.O.PRITCHARD
Distinguished Research Professor of Chemistry,
York University

R.W.NICHOLLS
Distinguished Research Professor of Physics
York University

and

M.W.P.CANN
Senior Project Scientist
CRESS, York University

Work on this project was conducted under the auspices of the Canada Centre for Mineral and Energy Technology, Energy, Mines and Resources, Canada

DSS FILE NUMBER: 41ST.23440-6-9162

DSS CONTRACT SERIAL NUMBER: 23440-6-9162/01-ST

CANMET PROJECT NUMBER: 502002

CANMET SCIENTIFIC AUTHORITY: M.V.C. Sekhar

63pp

Feb 15 1988

MICROMEDIA

CONTENTS

	Page
ABSTRACT	3
1: INTRODUCTION	4
1.1 Statement of Work	4
1.2 Procedures used to undertake the tasks	6
1.3 Personnel	6
2: DEFINITION OF THE PROBLEMS AND SCOPE OF WORK	7
3: IGNITION STUDIES	7
4: DEHYDROGENATION OF AROMATICS IN THE GAS PHASE	9
5: THERMODYNAMIC AND KINETIC COMPUTATIONS	13
6: DEVELOPMENT OF EXPERIMENTAL METHODOLOGY	18
6.1 Ignition	18
6.2 Dehydrogenation	18
6.3 An Alternative Solution	19
7: CONCLUSIONS	22
APPENDIX 1 (M.W.P.Cann) SHOCK TUBE DESIGN	A1-1 to A1-22
APPENDIX 2 (M.W.P.CANN) SHOCK TUBE DIAGNOSTICS	A2-1 to A2-18

ABSTRACT

In the context of the aromatic and napthenic contents of synthetic crudes from the Canadian Oil Sands and the need to make them more acceptable for the production of diesel and jet fuels, a search of the literature was made to assess the present state of knowledge of the properties of polyaromatic hydrocarbons in respect of (i) rates of ignition of mixtures with air and (ii) rates of dehydrogenation during the early stages of the ignition and combustion processes.

Relevant thermochemical calculations on these topics were undertaken.

An analysis was then made of the feasibilty of an experimental study of these two problems by shock-tube methods, and the conditions required were defined.

The shock-tube approach would require the use of the laser-based CARS (coherent anti-stokes raman spectroscopy) as a diagnostic tool.

An alternative approach would be to perform experiments using a compression-ignition research facilty or the V(ery) L(ow) P(ressure) P(yrolysis) method.

1: INTRODUCTION

1.1 Statement of Work and Objectives

The objectives and work statement of the contract are:

OBJECTIVES:

The objective of this contract is quantatitively to assess the extent of dehydrogenation reactions that might occur in pre-and post-combustion zones of a jet engine when hydrogenated syncrude distillates are used in jet fuels. This will be accomplished by computing the competitive kinetic rate constants for dehydrogenation and combustion of selected napthenic compounds normanlly found in jet fuels derived from syncrudes.

It is anticipated that not all relevant kinetic and thermodynamic data can be theoretically computed and that some experimental work needs to be conducted using high temperature techniques such as shock tubes. A second objective of this contract is therefore to establish the nature and extent of further experimental work.

WORK STATEMENT

Task 1: Definition of the Problem and scope of the work

The objective of this task is to identify in more specific detail, based on the present state of knowledge, the extent of the problem posed by the use of syncrude fuels in jet engines. A critical and thorough survey of the relevant current literature should be conducted to determine and develop a plan of attack. The literature examination should be conducted so as to aid in the selection of model compounds to be included in this study. The intent of the task is to define explicitly and in detail what can and what cannot be done.

Task 2: Thermodynamic and kinetic computations

A large body of data is available pertaining to thermodynamic properties of a large number of pure compounds known to be present in jet fuels. Techniques are further available for estimating these properties where such data do not exist. Extensive use of these and other methods will provide a solid

ground for estimating the stability and reactivity of the problem components. Once this is done it is possible to predict the extent of dehydrongenation vis-a-vis combustion of the problem components in a jet engine environment. This task thus involves the collection and evaluation of kinetic and thermodynamic data for a number of model components typically known to be present in jet fuels.

Task 3: Development of experimental methodology

The results from Task 2 are expected to provide a basis for deciding on the direction for further experimental work. Under this task, the current literature pertaining to using shock tube techniques for studying combustion and dehydrogenation kinetics will be critically reviewed. The task also involves the selection of a set of model compounds for experimental investigation using a shock tube. The contractor is then expected to define the scope of the experimental work feasible using shock tube techniques.

Task 4: Reports and Seminars

Monthly reports will be submitted by the contractor which will include progress achieved to date in each task and the amount of monies spent.In addition the monthly report will highlight any significant results obtained during the report period. The objective of these reports is to provide sufficient information to the Scientific Authority to assess the progress of the contract in terms of results obtained and to make any necessary modifications.

A draft final report will be submitted at the end of task 3. The report will be prepared in accordance with good engineering practices and will include as a minimum:

a) List of Contents

b) Summary or abstract

c) Introduction

d) Complete description of the work undertaken

e) Technical discussion

f) Conclusions

g) Supporting graphs, table and figures

After approval of the final draft report, the original and ten copies of the final report will be submitted.

Seminar: By arrangement with the Scientific Authority, the contractor will provide a debriefing seminar in Ottawa or at any other suitable location for the benefit of the public and the industry.

1.2 Procedures used to undertake tasks

In the spirit of the work statement, H.O.Pritchard spent the first few months of the contract assessing the state of knowledge from the literature in the field. That work is reviewed in sections 2, 3 and 4 below. Supporting thermodynamic calculations were then undertaken by him, as described in section 5. Experimental methodologies for ignition and dehyrogenation studies derived from these calculations are reviewed in section 6.

At this stage, M.W.P.Cann, with whom the potential for shock tube experiments were discussed, made an assessment of this problem. The requirements for a shock tube to be used to provide the information called for in the work statement is reviewed by him in Appendix 1 (Shock Tube Design). He then reviewed some of the optical/spectroscopic diagnostic methods that might be used if a shock tube approach were adopted, and these are reviewed in Appendix 2 (Shock Tube Diagnostics) He points our that the Coherent Anti-Stokes Raman Spectroscopy (CARS) method shows great promise for a shock tube approach.

Two solutions to each problem are proposed in Section 7. To measure ignition rates, either Shock Tube or Compression Ignition methods could be used. To meaure dehydrogenation rates, either Very Low Pressure Pyrolysis methods or Shock Tube methods augmented by Coherent Anti Stokes Raman Spectroscopy could be used. It is possible that the shock tube studies could be made at York, but the existing facilities would need to be enhanced to include a CARS detection system.

1.3 Personnel

The personnel who carried out this study are:

Prof. H. O. Pritchard
Chemical, Thermochemical and Combustion considerations

M.W.P.Cann
Shock Tube Methodology and Diagnostics

Prof. R.W.Nicholls
Project Management, Shock Tube Spectroscopy

2: DEFINITION OF THE PROBLEM AND SCOPE OF THE WORK

The problem of interest is the poor quality of diesel and jet fuel fractions derived from Alberta oil sands, which is associated with the high aromatic content of these liquids[1]. The questions that we were asked to address were

1) the correlation of ignition characteristics as a function of aromaticity

2) the ease with which saturated polycyclic ring compounds might dehydrogenate back to aromatic species - for example, if this process were to be very facile, it would render useless any hydrogenation process that the fuel had undergone in order to reduce its aromaticity.

An important aspect of aromatic combustion that we were not asked to consider - one which is (and has been for a long time) very active, is that of soot formation: this is important both for diesel engines and jet engines.

It was also implicit in the original request that we would expect to be able to solve these problems by shock-tube measurements.

3: IGNITION STUDIES

Shock-tube ignition studies may be divided into two classes:
(1) the rates of ignition of simple hydrocarbons like methane e.g. refs. [2] [3]; the former studied the light emission, with a view to characterising some of the transient carbonyl species; the latter was aimed at the general understanding of small-molecule combustion, and the associated cool flame phenomena.

---

[1] M.F. Wilson, "Impact of excessive aromatics in oil sand syncrudes on production and quality of middle distillate fuels". CANMET Report 82-2E 1981.
[2] C.R. Orr, 9th Symposium (International) on Combustion, p.1043 (1963).
[3] T. Asaba, K. Yoneda, N. Kakihara and T. Hikita, ibid. p.193.

(2) In the present context, Kling and Maman[4] studied the shock ignition of "aviation kerosene"/air mixtures. The kerosene was confined by a diaphragm in a separately heated section of the shock tube at about 200°C, and this diaphragm was burst by the incident shock wave. This raised the temperature to about 550°C and the reflected shock then took the temperature to about 970°C, where ignition took place in about 1.5 ms for equivalence ratios (ϕ = molar fuel: oxygen ratio, scaled to ϕ = 1 as stoichiometric) of about 6-10. They also quote an earlier paper by Mullins[5], which taken together with their work, shows that the ignition delay declines to about 500 μsec for ϕ = 3 and 100 μsec for ϕ = 1 at 1 atm total pressure. In a diesel engine, we are interested in ignition at temperatures in the region 300°C (cold start) to 600°C (full load) at pressures of about 30-50 atm, and equivalence ratios of between 0.5 and 1. In a jet engine (JT8D), on the other hand[6], we are concerned with an induction period of about 700μsec., during which the temperature of the fuel-air mixture rises from about 400°C to 700°C, whereupon ignition commences. Temperature coefficients for ignition of n-heptane (measured for equivalence ratio of 1, diluted to 3% in Argon, at 3-20 atm total pressure) give[7] the ignition delay in seconds as 10^{-7} $\rho^{-1.8}$ $e^{30000/1.987T}$ where ρ is in atmospheres, near 970°C ~ 1240°K: therefore, at 620°K ~ 350°C, which is close to the temperatures found at cold start in a diesel engine, and the ignition time would be about 2 x 10^5 times as long as the figures quoted by Kling and Maman at 1 atm, or ~ 100 times as long at 40 atm, i.e. ~ 10 msec. In a diesel engine operating at 2000 rpm, we are interested in ignition times near 1 msec.

---

[4]R. Kling and A. Maman, 8th Symposium (International) on Combustion, p.1096 (1962)
[5]B.P. Mullins, Fuel, 32, 234 (1953).
[6]R.A. Craig and H.O. Pritchard, Can. J. Chem. 55, 1599 (1977).
[7]A.A. Barisov, S.M. Kogarko and A.V. Lyumbimov, Zhur. Priklad. Mekhan; Tekh. Fiz. 3, 175 (1960).
[8]R.D. Wilk, R.S. Cohen and N.P. Cernansky. 20th Symposium (International)

Consistent with these estimates is the measurement of cool-flame induction times in dodecane at 523-623°K (i.e. 250-350°C, close to our desired lower limit) of 1-2 secs at 400 Torr[8]; they also showed, as expected, that the addition of tetralin increases the ignition delay.

We found no direct shock-tube studies of ignition of prototype molecules under diesel engine or jet-engine preignition conditions, and in a later section, we address the problem of such measurements.

4: DEHYDROGENATION OF ATOMATICS IN THE GAS PHASE

Whereas the reversible dehydrogenation of cyclohexane to cyclohexene[9] over (usually platinum) catalysts at about 200°C must be the most studied chemical reaction of all (2 or 3 columns of entries in Chemical Abstracts each year!), work on homogeneous dehydrogenation of cyclic hydrocarbons is almost non-existent. At the beginning of this contract, it had been our intention to collect rate data on sequential processes e.g.

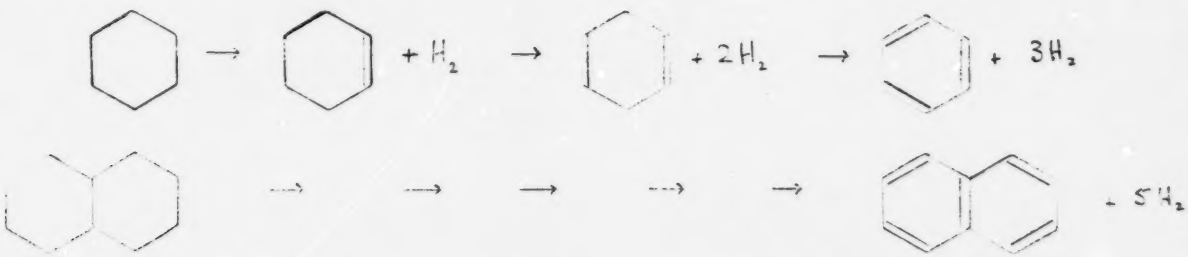

and solve for the overall rate at temperatures of interest by standard differential-equation techniques[10], but upon searching the literature, it was impossible to find sufficient examples of these dehydrogenation reactions - to

[9] Kirk-Othmer Encyclopaedia of Chemical Technology, 3rd Edition, Volume 12, pp 931-937.

[10] e.g. D.L.S. McElwain and H.O. Pritchard. J. Amer. Chem. Soc. 91, 7963 (1969).

the extent that it wasn't even possible to make educated guesses which could be fed into the calculation.

There are ample data on variants of the dehydrogenation of 1,4-cyclohexadiene[11] [12], as follows

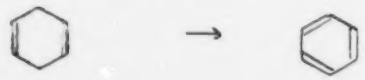

log A = 12.0(s^{-1}) E = 42.5 kcal.mol^{-1}

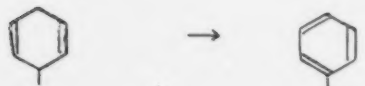

12.5 43.0

12.1 40.0

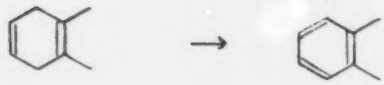

12.5 43.7

13.1 45.9

13.0 48.5

12.8 49.9

14.2 52.5

However, there is little else: for the 1,2-cyclohexadiene, there are only two results[12], which agree reasonably in the observed temperature range, viz.

14.1 61.6

13.4 59.0

[11] P.J. Robinson and K.A. Holbrook, Unimolecular Reactions, John Wiley, 1972.
[12] P.J. Robinson. Specialist Periodical Reports, Reaction Kinetics, 1, 145 (1975).

and only one measurement of the dehydrogenation of cyclohexene (actually tetra-deutero-cyclohexene)[13]

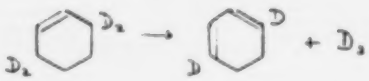

12.6 61.6

The reaction does not appear to occur homogeneously in the gas phase. Extensive shock-tube studies[14] show that the initial step in the decomposition of cyclohexane at temperatures near 1100°K (i.e. ~ 800°C) is the isomerisation to 1-hexene (linear chain), followed by break-up to ethylene and butadiene. At these same temperatures, Tsang also finds [15] that the principal reaction of cyclohexene is also to give ethylene and butadiene, in contrast to the results at lower temperatures in reference 13.

The situation with the two-ring compounds, i.e. the dehydrogenations in the sequence (decalin → tetralin + $3H_2$ → naphthalene + $5H_2$) is similar, only worse. Again, there are thousands of papers on the catalytic dehydrogenations, ending up at naphthalene, or else at partially dehydrogenated intermediates, but nothing in the homogeneous phase.

There have been two cursory studies of the dehydrogenation of tetralin to naphthalene in the gas phase[16] [17]: the former simply quotes an overall rate for the temperature range 500-670°C in 1st order form, as $k = 2 \times 10^{16} e^{-72300/1.987T}$ which has a value of 7×10^{-8} s^{-1} at 400°C - VERY SLOW! In the other study, Gangwer et al. actually isolated the intermediate, i.e.

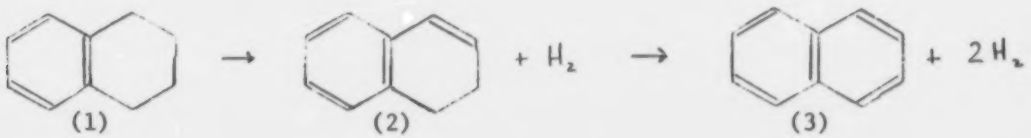

(1) (2) (3)

[13]D.C. Tardy, R. Ireton and A.S. Gordon, J. Amer. Chem. Soc., 101, 1508 (1979).
[14]W. Tsang, Int. J. Chem. Kinetics, 10, 1119 (1978).
[15]W. Tsang, J. Chem. Phys. 42, 1805 (1965).
[16]H. Tominaga, N. Yahagi and M. Ishiwatari, J. Fac. Eng. Univ. Tokyo, 15, 68 (1977); C.A. 89, 128862n.
[17]T. Gangwer, D. MacKenzie and S. Casano. J. Phys. Chem. 83, 2013 (1979).

[note that the alternative intermediate 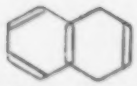 was not found]. They concluded, on reasonable but not unequivocable evidence, that these reactions, although performed under vacuum conditions in a quartz flask, were heterogeneous, and they expressed them as zero-order rate constants with a dependence on surface area. They only worked at 400°C, which is in our range of interest - at least for diesel ignition - and if their rates are expressed (for comparison with the Japanese study) in first-order form, they are 1×10^{-6} s^{-1} for step (1) → (2) and 3×10^{-6} s^{-1} for step (2) → (3), which converts to approximately 3×10^{-8} s^{-1} for the overall process.

This number was calculated by a very crude steady-state approximation:

If the process is $T \underset{k_{21}}{\overset{k_{12}}{\rightleftharpoons}} D \xrightarrow{k_{23}} N$ with $k_{12} = 1 \times 10^{-6} s^{-1}$ and $k_{23} = 3 \times 10^{-6} s^{-1}$

then $R_D = k_{12}[T] - (k_{21}+k_{23})[D] = 0$ i.e. $[D] = k_{12}[T]/(k_{21}+k_{23})$:

thus, the overall rate constant is $\bar{k} = [T]^{-1} R_N = [T]^{-1} k_{23}[D] = k_{12}.k_{23}/(k_{21}+k_{23})$ This assumes that $[H_2]$ is large and constant. We need k_{21}, which is derived from the equilibrium constant between T and D, which we have assumed to be the same as that between cyclohexene and cyclohexadiene: from Table 2, the value for 675°K is interpolated to be very close to 10^{-2}, whence $k_{21} = 100\ k_{12}$; thence $\bar{k} = 1 \times 10^{-6} \times 3 \times 10^{-6}/(100 \times 10^{-6} + 3 \times 10^{-6}) = 3 \times 10^{-8}$ s^{-1}. Thus, it would seem that the two sets of measurements on this reaction are reasonably consistent, although they have been interpreted quite differently.

One recent study of the rate of decomposition of decalin in a quartz tabular reactor[18] shows a rate of disappearance of 0.5 s^{-1} at 700°C, to be compared with a rate of dehydrogenation of tetralin[16] of 1.1 s^{-1} at the same temperature; however,

[18]W.A. Rubey, S.L. Mazer, P.H. Taylor and J.G. Stalter, ACS Symposium on The Structure of Jet Fuels, Colorado, April 5-10, 1987, Preprints, p.526.

it is not clear that this is to be interpreted as the rate constant for dehydrogenation of decalin since the mechanism was not established, only that the products were benzene > toluene > styrene > naphthalene > indene > xylene. Nevertheless, it must be an upper limit, confirming that dehydrogenation of decalin is also quite slow at all temperatures of interest in the early ignition stages for both diesel- and jet-engine combustion.

All the evidence seems to point to the fact that these dehydrogenation reactions are exceedingly slow on engine time scales, and one should seriously consider whether or not in fact, they may occur heterogeneously in the engine. It is easy to see how this could happen in a diesel engine, since there will always be particulate matter of graphitic type present in the compression, which could facilitate the dehydrogenation. It is harder, however, to see how such a mechanism could occur in the early stages of combustion in a jet engine, where the ignition phase of the combustion should be homogeneous - unless, perhaps, there is sufficient metallic content in the fuel itself to act as a catalyst for the dehydrogenation.

5: THERMODYNAMIC AND KINETIC COMPUTATIONS

Reliable thermodynamic data exist for the sequence of molecules: cyclohexane, cyclohexene, cyclohexadiene (both isomers) and benzene[19] [20] and there is no doubt that at the temperatures of interest, the equilibrium lies well over towards the aromatic species, benzene, as is shown in Tables 1 and 2.

[19]W.J. Taylor, D.D. Wagman, M.G. Williams, K.S. Pitzer and F.D. Rossini. J. Res. Natl. Bur. Stand. 37, 95 (1946).
[20]O.V. Dorofeeva, L.V. Gurvich and V.S.Jorish, J. Phys. Chem. Ref. Data, 15, 437 (1986).

Such extensive data do not exist for polynuclear aromatic molecules and we have to resort to "bond additivity" methods for estimating the enthalpy data[21], which are very reliable these days. We use here the method of Laidler, which works extremely well for fused hydrocarbons in general (i.e. alkanes, cycloalkanes, alkenes, alkylbenzenes and aromatics). For fused aromatics, the contributions to the heat of atomisation are

$E(C_b\text{-}H)$ = 100.53 kcal.mol^{-1}

E(-CH-CH-) = 119.17

E(-CH-C=) = 114.30

E(=C-C=) = 112.80

For alkylbenzenes, one needs in addition

$E(C_b\text{-}C)$ = 88.91 kcal.mol^{-1}

and the data for alkanes, viz.

$E(C\text{-}H)_p$ = 98.19 kcal.mol^{-1}

$E(C\text{-}H)_s$ = 97.27

$E(C\text{-}H)_t$ = 96.53

E(C-C) = 85.48

Thus, the heat of atomisation of cyclohexane is 6 x 85.48 + 12 x 97.27 = 1680 kcal.mol^{-1}, and for benzene, is 6 x 119.17 + 6 x 100.53 = 1318 kcal.mol^{-1}. These figures, taken together with the standard values of $\Delta H_f(H)$ = 52.10 and $\Delta H_f(C)$ = 170.90 kcal.mol^{-1} then lead to the standard heats of formation of the substances of interest, viz

[21] eg J.D. Cox and G. Pilcher, Thermochemistry of organic and organometallic compounds. Academic Press, 1970, Chapter 7.

$$\Delta H_f(\text{molecule}) = \Sigma\ \Delta H_f\ (\text{atoms}) - \Sigma H_{\text{atomisation}}$$

e.g. ΔH_f(cyclohexane) = 6x170.90 + 12x52.10 - 1680 = 1651 - 1680 = -29 kcal.mol^{-1}

ΔH_f(benzene) = 6x170.90 + 6x52.10 - 1318 = 1338 - 1318 = +20 kcal.mol^{-1}

The observed values are -29.5 and +19.8 kcal.mol^{-1} respectively.

In Table 3, we compare the enthalpy of formation and of dehydrogenation for the cyclohexane → benzene series and the decalin → naphthalene series. It can be seen that on going from decalin to tetralin, the enthalpy pattern is virtually the same as that for cyclohexane to benzene. This pattern then has to be modified (since it takes now only the loss of $2H_2$ to complete the next aromatic ring), but will always show a large ΔH for removal of the first H_2 from the shared ring, and a much smaller ΔH to complete the additional aromatic ring - note that the ΔH to remove $2H_2$ from tetralin is the same as that needed to remove $1H_2$ from decalin. These patterns persist throughout the whole family of polynuclear aromatic reaction systems.

TABLE 1

Equilibrium constants for the dissociation of cyclohexane in steps as far as benzene

Log_{10} (Equilibrium constant of formation)

	500°K	600°K	700°K	800°K	900°K	1000°K
	-14.943	-17.489	-19.373	-20.819	-21.958	-22.873
	-19.700	-20.099	-20.441	-20.728	-20.967	-21.166
	-24.727	-23.122	-22.019	-21.216	-20.605	-20.122
	-25.382	-23.733	-22.601	-21.777	-21.150	-20.656
	-17.152	-15.904	-15.052	-14.435	-13.972	-13.609

TABLE 2

Equilibrium constants for the dissociation of cyclohexane in steps as far as benzene

Log_{10} (Equilibrium constant of formation with respect to cyclohexane)

	0.0	0.0	0.0	0.0	0.0	0.0
	-4.757	-2.610	-1.068	+0.091	+0.991	+1.707
	-9.784	-5.633	-2.646	-0.397	+1.353	+2.751
	-10.439	-6.244	-3.228	-0.958	+0.808	+2.217
	-2.209	+1.585	+4.321	+6.384	+7.968	+9.264

TABLE 3

Heats of formation and dehydrogenation of cyclohexane and decalin

(the underlined heats of formation are estimated by Laidler's method)
(units of kcal.mol^{-1})

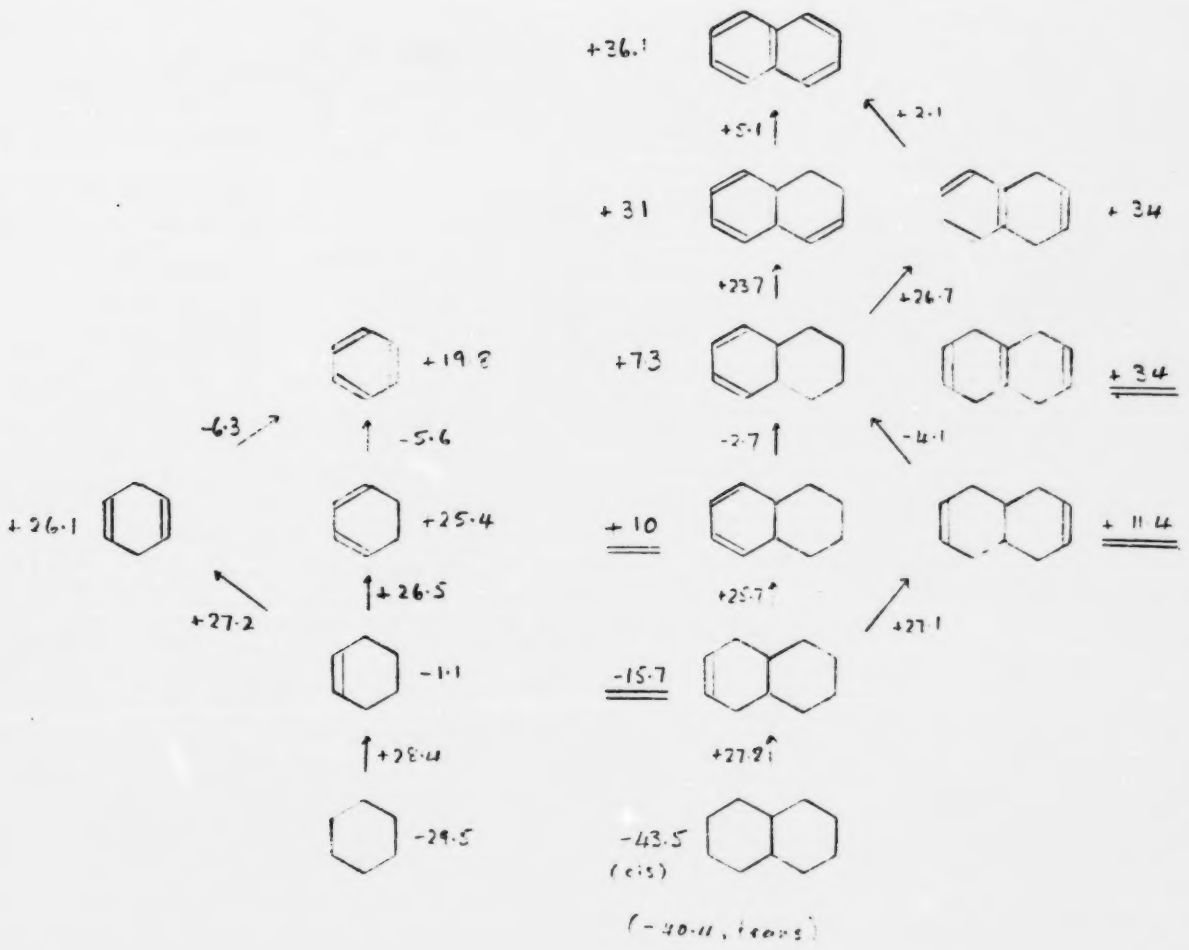

Note: in each sequence, the vertical path is the most favourable one

The position in regard to the calculation of entropies for these 2-ring compounds is much less satisfactory. Values have been estimated at 300°K for several 2- and 3-ring compounds[22], but these calculations are based on group additivity concepts (which are much less well tested than group additivities for ΔH), rather than upon spectroscopic data as in the 1-ring case above; thus, extrapolation to any other temperature is questionable. Something nearer to what is required has been done by Cyvin[23] for naphthalene, anthracene and phenanthene, whose entropies at several temperatures up to 500°K are given: the major problem here is the extreme difficulty in making vibrational assignments for N-atom molecules when N is large and there is no symmetry to simplify the analysis.

For the time being, until fine details of a given process are needed, we can argue that in the process

$$RH_2 \rightarrow R + H_2$$

the contributions to the entropy change are, in order of magnitude:

creation of $S_{trans}(H_2)$

creation of $S_{rot}(H_2)$

creation of $S_{vib}(H_2)$ - at elevated temperatures only

loss of 6 S_{vib}(C-H) components between RH_2 and R

small loss in S_{trans} going from RH_2 to R

small loss in S_{rot} going from RH_2 to R

Since the dominant terms are the creation of $S_{trans}(H_2)$ and $S_{rot}(H_2)$ for all cases, one can simply take ΔS to be the sum of these two terms, regardless of the reaction, and in fact, in the first instance, values from the cyclohexane → benzene sequence could be used.

[22]R. Shaw, D.M. Golden and S.W. Benson, J. Phys. Chem. 81, 1716 (1977).
[23]O.V. Dorofeeva, L.V. Gurvich and C.J. Cyvin, Thermochimica Acta, 102, 59 (1986).

6: DEVELOPMENT OF EXPERIMENTAL METHODOLOGY

For direct comparison with conditions that occur in both diesel and jet engines we require air pressures in the range of 15-40 atm and temperatures in the range of 300-700°C; moreover, we require that ignition shall take place within a time of about 1 msec[6] [24], or a little less. It turns out to be difficult to achieve these conditions in a shock tube (the lower the temperature or the higher the pressure, the worse it is), as is shown in Appendix I: there, we examine the slightly easier problem of achieving temperatures in the range 400-800°C at 20 atm, and it is shown that although feasible, the cost in driver gases could be considerable. At this point, we should divide the discussion into two aspects: ignition and dehydrogenation.

6.1: Ignition

The ignition is the easier problem, by far; ignition is accompanied by light emission, which is easily detected (and also by large changes in pressure and temperature), and the only tricky choice would be that of how to introduce the hydrocarbon sample into the gas flow - there would seem to be three alternatives (i) a heated section of shock tube, as was used in reference 4; (ii) ablation from a drop of liquid suspended from a hypodermic needle in the shock flow; (iii) a Bosch-type diesel injector, triggered to coincide with the firing of the shock tube. Method (iii) would appear to be the most difficult, and the choice would really be between (i) and (ii).

[24] C.L. Wong and D.E. Steere, S.A.E. Technical Paper 821231 "The Effects of diesel fuel properties and engine operating conditions on ignition delay" 1982

6.2: Dehydrogenation

This problem suffers from the additional complication in respect of detection. The H_2 formed is optically transparent, and can only be detected by modern laser techniques (see Appendix II); moreover, the spectra of the hydrocarbons formed are insufficiently unique to be able to give any meaningful results - e.g. the u.v. spectra of naphthalene and di-hydro-naphthalene are so similar that one could not base a quantitative analysis on the differences. A method that could be envisaged - with great difficulty and expense - is that of the dump tank, with v.p.c. analysis for the resulting H_2; however this approach would deny the possibility of achieving the required temperatures and pressures in a reflected shock, and compound the difficulties described in the Appendix I. Another alternative might be to sample the reflected shock with a mass spectrometer for H_2, but again, this would be a very formidable experiment. On balance, the direct shock tube approach using reflected shocks and CARS detection methods, as described in Appendix II, would seem to be the best approach. There are several shock-tube facilities in this country, but as far as we know, none is equipped with a CARS diagnostic facility: thus, in order to study the dehydrogenation problem in a shock tube, one is faced with the purchase of laser equipment whose cost will be in the $50-100K range.

6.3: An Alternative Solution

To be meaningful, ignition studies would have to be carried out under realistic engine conditions, as enumerated at the beginning of this section. This can be fairly easily achieved in a single pulse rapid compression ignition machine[25 27]: ignition could be detected either by light emission or by pressure

[25]P. Beeley, P. Gray and J.F. Griffiths, 17th Symposium (International) on Combustion, 1979, p.1415.
[26]J.F. Griffiths and A. Perche, 18th Symposium (International) on Combustion 1981, p.893.
[27]J.F. Griffiths and S.M. Hasko, Proc. Roy. Soc. London A393, 371 (1984).

change - both have been used in the cited studies. The only unsolved problems are (a) that of introducing the relatively involatile fuels in sufficient quantity so as to achieve the desired equivalence ratio - it would have to be one of methods (i)-(iii) itemised in the subsection above; (b) constructing a larger and more robust machine so as to be able to stand the higher pressures of interest here.

On the other hand, dehydrogenation is a fundamental chemical kinetic reaction, and rate constants measured in one regime are directly transferable to other conditions of temperature and composition - hence there is no over-riding need to study these reactions in a shock tube, nor, for that matter, even in a compression device of any kind. For cyclohexane, a possible approach would be to undertake some relatively conventional kinetic studies in the 400-600°C range to see whether the homogeneous dehydrogenation reaction has been overlooked although this seems most unlikely. For tetralin, it has already been alleged that the dehydrogenation is heterogeneous, although this is not entirely certain[17]. It would appear that a viable approach to the solution of this problem might be to use the VLPP (very low pressure pyrolysis) technique, in which the ratio of gas-gas to gas-wall collisions can be controlled, and hence heterogeneous versus homogeneous contributions can be evaluated. The method was developed by S.W. Benson and D.M. Golden[28] and was extensively used for about a decade.

We are not aware of anyone in this country who has either a compression ignition machine nor a VLPP machine, and if it is wished to expedite these studies by non-shock tube means, they might most easily by done by letting contracts to people outside the country: J.F. Griffiths in Leeds, England is interested in hydrocarbon ignition, and may well be willing to collaborate in the suggested studies; for the VLPP experiment, it appears that the only currently operating machine is that of K.D. King in Adelaide, Australia.

---

[28]K.D. King, D.M. Golden, G.N. Spokes and S.W. Benson, Int. J. Chem. Kinetics 3, 411 (1971).

7: CONCLUSIONS

This study revealed that very little information exists in the literature either on the rates of ignition of polynuclear aromatic hydrocarbons or on the rates of their dehydrogenation, especially the latter.

The only ignition studies which were located refer to a temperature regime far removed from that appropriate to a diesel engine, but extrapolation to the diesel regime gives sensible ignition delay times.

This approach could be extended to the study of ignition rates of certain certain prototype polynuclear aromatic hydrocarbons using shock tube methods. The major difficulty, expected in the use of shock tubes, is, as described in Appendix 1, the problem of achieving the appropriate temperatures and pressures in the shock for reasonable driver pressures. As pointed out in Appendix 1, use of reflected shock waves and argon-buffered nitrogen as the driver would probably overcome these difficulties.

An alternative approach to these prolems would be to use a compression ignition machine.

It was pointed out in Appendix 2 that species detection and measurement is an additional problem to be overcome when using shock tube methods to measure rates of dehydrogenation, of hydrogenated polynuclear aromatics. It is further shown in Appendix 2 that this problem may be overcome by the use of the elegant Coherent Anti Stokes Raman Spectroscopy (CARS) method.

An alternative to this approach might be to adopt a more traditional chemical kinetic approach such as use of the Very Low Pressure Pyrolysis (VLPP) method.

Neither the compression ignition nor the VLPP expertise is available in this country, but the shock-tube and laser expertise required the CARS method is.

The principal recommendation of this study is that the CARS diagnostic method be used in shock tube experiments to determine the rates of dehyrogenation of prototype hydrogenated polynuclear aromatics.

Appendix - 1. Shock Tube Design

M.W.P.Cann

		Page
1.	REQUIREMENTS	1
2.	GENERAL SHOCK TUBE CHARACTERISTICS	1
	Rankine-Hugoniot Relations	3
3.	DRIVER PRESSURES	4
	Incident Shock Waves	4
	Reflected Shock Waves	6
4.	TEST TIME	7
	Incident Shock Waves	9
	Reflected Shock Waves	11
	Results	12
5.	HEATED SHOCK TUBE	14
6.	CONCLUSIONS	15
References		17
Table 1. Shock Wave Conditions		18
Table 2. Driver Pressure Ratios		19
Table 3. Conditions Behind Reflected Shock Waves		20
Figure A1-1.	(x,t) Shock Tube Diagram - Incident Wave Study.	21
Figure A1-2.	(x,t) Shock Tube Diagram - Reflected Wave Study.	22

---

1. REQUIREMENTS

A shock tube is required to study dehydrogenation and combustion onset in organic compounds, such as benzene, cyclohexane, cyclohexene. The required experimental conditions are the following:

Temperatures	400 to 800 C
Pressure	20 atmos.
Test times	0.0001 to 0.001 sec.
Test gas	air, or inert gas plus oxygen, with small quantities of organic compound

2. GENERAL SHOCK TUBE CHARACTERISTICS

Figure A1-1 is the (x,t) diagram of a shock tube showing the wave history after diaphragm rupture. The numbers identifying the various regions are used below in the discussion and calculation of properties of these regions and are:

1 undisturbed working region, prior to shock wave arrival

2 working region behind incident shock wave

3 driver gas cooled and accelerated by diaphragm rupture

4 undisturbed driver gas - at conditions prevailing before diaphragm rupture

5 region behind the reflected shock wave, which has reflected off the end wall of the working region.

The figure shows how the test time at some station A begins with the passage of the shock wave and terminates with the arrival of either

the contact "surface", which marks the junction of driver and driven gases, the former cooled and the latter heated, or the rarefaction wave from the end of the driver section, whichever comes first. The rarefaction wave travels at sound speed in the moving gas of regions 3 and 2, which are subsonic relative to the shock front, so that given enough time it will eventually catch up with the shock front.

Other points to bear in mind are that the shock wave does not form immediately upon diaphragm rupture but at some distance downstream, reaching peak strength at some 30 diameters distance. Secondly, the contact "surface" is a region of turbulent mixing and is more extensive than one-dimensional theory suggests, thus reducing the available observing time. Thirdly, the shock wave first accelerates as it gains strength and then decays, due to boundary layer growth and leakage past the contact region in the boundary layer. In this study the boundary layer is ignored and so is the formation time of the shock wave, i.e. all diaphragm effects, petalling, opening time etc. are ignored. Qualitative recognition is made of the diffuseness of the contact region by applying an uncertainty factor to estimated observation times.

Observations in the shock tube may be made behind the incident wave or behind the shock wave reflected from the end wall of the working section. These provide somewhat different conditions.

(a) Incident shock wave.
Passage of the shock wave accelerates the gas through which it passes. Thus an observer at A monitors gas samples which are changing with time as the gas is swept passed the station. This is satisfactory if the gas is uniform but not otherwise. Here the lapsed time, time since a particular gas sample passed through the

shock wave is the time since the shock wave pased A multiplied by the density ratio (ρ_2/ρ_1).

(b) Reflected shock wave.
The return shock brings the gas to rest so that the observer at B, Figure A1-1, follows the same gas sample throughout the observation period. Other advantages of making observations in the reflected shock region are the increased pressures and temperatures obtainable (stagnation conditions) for moderate incident shock strengths and sometimes a longer observing time as the reflected shock wave moves to meet the approaching contact region and rarefaction wave. The events following these meetings may be various with transmitted or reflected disturbances but under some conditions (tailored interface) the reflected shock and contact region can both come to rest, thus further increasing the test time.

Calculations are now made for these two situations. It is assumed that the working medium is either air or a mixture of 21% O_2 and 79% argon - in fact the working medium will be treated as air or argon, for simplicity. Using argon as a buffer gas offers stronger shocks at lower pressures but also preempts the formation of oxides of nitrogen, which occur in air.

Rankine-Hugoniot Relations

These equations are derived from the conservation expressions in one-dimension for energy, momentum and continuity. They are,

$$\frac{P_2}{P_1} = \frac{2\gamma_1 M_1^2 - (\gamma_1 - 1)}{\gamma_1 + 1} \qquad [1]$$

$$\frac{\rho_2}{\rho_1} = \frac{(\gamma_1 + 1)\, M_1^2}{(\gamma_1 - 1)\, M_1^2 + 2} \qquad [2]$$

and from the perfect gas law

$$\frac{T_2}{T_1} = \frac{P_2}{P_1}\,\frac{\rho_1}{\rho_2} \qquad [3]$$

The pressure of gas in the driver section which produces a shock of strength M_1 is obtained from

$$\frac{P_4}{P_1} = \left[\frac{2\gamma_1 M_1^2}{\gamma_1 + 1} - \frac{\gamma_1 - 1}{\gamma_1 + 1}\right] \Bigg/ \left[1 - \frac{\gamma_4 - 1}{\gamma_1 + 1}\,\frac{a_1}{a_4}\left(M_1 - \frac{1}{M_1}\right)\right]^{2\gamma_4/(\gamma_4 - 1)} \qquad [4]$$

where a_1, a_4 are sound speeds in regions 1 and 4 respectively. In practice [4] is not very accurate as it takes no account of such effects as diaphragm opening time, petalling and boundary layers, so that rather weaker shocks are observed. The equation is used here as a guide, with the understanding that the required pressure ratio may be as much as 50% higher.

3. DRIVER PRESSURES

Incident Shock Waves

Relations [1,2,3] were used to compute Table 1, which gives the conditions behind behind shock waves in monatomic and diatomic gases

(γ_1= 5/3 and 7/5 respectively) for specified shock Mach number M_1, expressed in terms of the sound speed in the unshocked gas, state 1. These gases may be argon and air, for example, and are assumed to be buffers with any other components, such as oxygen with the argon, being thermodynamically insignificant. For a temperature T_1=296K the required range in the ratio T_2/T_1 is from 2.27 to 3.63 and the table then gives the necessary range in shock Mach number as 2.0 to 3.0 for a monatomic buffer, and 2.6 to 3.8 for a diatomic buffer. Table 2 was constructed from [4] and shows the diaphragm pressure ratios required to generate shocks with various combinations of driver and driven gases.

Calculations for the temperature extrema can be made using Tables 1 and 2. The initial temperature of both working and driver gases is assumed to be 296K,

Buffer	M_1	P_2/P_1	P_1 (atm)	Driver	P_4/P_1	P_4 (atm)	P_4 (psia)
argon	2.0	4.75	4.211	argon	49.8	209.7	3,083
				nitrogen	23.8	100.2	1,473
				helium	8.93	37.6	553
	3.0	11.0	1.818	argon	2,673	4,859	71,434
				nitrogen	205.6	1,234	18,137
				helium	35.9	65.3	960
air	2.6	7.72	2.591	nitrogen	182.9	473.9	6,966
				helium	25.1	64.9	954
	3.8	16.68	1.199	nitrogen	7,326	8,784	1.309+5
				helium	128.2	153.7	2260

If one is constrained to normal bottled gases (2,600 to 2,800 psia) then the pressures shown above will give only one, or at most two, shocks per bottle of gas, and then only with helium driving argon. Small bore shock tubes might improve this slightly but either way the cost would be high. Recalling that the above pressures are obtained from [4], and therefore represent the lower limit in each case, it is then clearly unrealistic to consider generating the experimental conditions behind incident shock waves, so reflected shocks must be considered.

Reflected Shock Waves

When the incident shock wave, travelling at Mach number M_1, is reflected off the end wall of the shock tube it travels back up the tube bringing the gas to rest, then converting the energy of motion into increased enthalpy. This means that the desired experimental conditions can be obtained with weaker incident shocks than would otherwise be required. The calculations start in the same way as before, since Table 1 is quite general, but now M is the Mach number of the reflected shock and the ratios are P_5/P_2, ρ_5/ρ_2, T_5/T_2 respectively. Table 3 was prepared as before but some of the numbers were generated by running the NASA Lewis Rsearch Center's chemical equilibrium computer program CEC72, as a less tedious alternative to hand calculation. This program also allows one to investigate the effect of gas mixtures quite easily, and to repeat calculations for different conditions.

In Table 3 M_1 is still the Mach number of the incident shock wave. Thus it is seen that incident shock waves in the Mach number range of 1.4 to 2.2 and 1.8 to 2.8 are required for monatomic and diatomic buffers respectively. From Table 2 the required driver pressures are now as follows,

Buffer	M_1	P_5/P_1	P_1 (atm)	Driver	P_4/P_1	P_4 (atm)	P_4 (psia)
argon	1.4	4.33	4.619	argon	5.63	26.02	383
				nitrogen	4.39	20.28	299
				helium	2.91	13.43	198
	2.2	20.0	1.000	argon	102.0	102.0	1,499
				nitrogen	39.36	39.4	579
				helium	12.2	12.2	179
air	1.8	1.906	0.467	nitrogen	17.90	34.1	502
				helium	6.76	12.9	190
	2.8	42.9	0.467	nitrogen	325.0	151.7	2,230
				helium	33.5	15.6	230

These pressures are still high but are usable for either buffer. It may be possible to use a nitrogen driver with argon buffer; although this uses more gas it should be cost effective.

4. TEST TIME

The test time begins with the passage of the shock wave, incident or reflected, past the observing station. It is terminated by the

arrival at this location of another pressure wave or gas discontinuity, of which there are several. Figure A1-1 shows the incident shock wave followed by the contact region, which is itself followed by the rarefaction fan from the driver section. The tail of this fan is propagating towards the end of the driver, at the local sonic speed, but since the gas is moving into the working section this tail normally proceeds in that direction also, with a speed $u_3 - a_3$. The head of the rarefaction fan travels to the left in the figure, through stationary driver gas at room temperature, and is reflected at the end of the driver. Thereafter this rarefaction head is pursuing the shock wave, moving with speed $u_3 + a_3$. Since both temperature and gas velocity are changing throughout the fan the speed of the rarefaction head to the right is also changing, up until it reaches the tail. The method of characteristics can be used to give the position of the head of the rarefaction fan as a function of time after diaphragm rupture and it catches up with the tail at (X_1, t_1) where

$$t_1 = \frac{L_{dr}}{a_4}\left[\frac{2\,a_4 - (\gamma_4 - 1)(u_3 - a_3)}{(\gamma_4 + 1)\,a_4}\right]^{2(\gamma_4-1)/(\gamma_4+1)} \qquad [5]$$

at this time the tail of the expansion fan has travelled a distance

$$X_1 = (u_3 - a_3)\,t_1 \qquad [6]$$

where $u_3 = u_2$. Note that all velocities "u" are given here in the the laboratory reference frame. The distance-time history of these events

is shown in Figure A1-1. For $t>t_1$ the head of the rarefaction travels at constant sonic speed towards the contact region, which it eventually reaches at (X_2,t_2). Thereafter the wave is travelling at sonic speed a_2 and will, given time, catch the incident shock wave, which is subsonic with respect to the gas behind it.

Incident Shock Waves

The test time behind the incident shock wave is terminated either by the arrival of the contact region or the driver rarefaction wave. A rarefaction wave is always transmitted through the contact region and some reflected waves can also be expected. For calculation purposes it simplest to assume that the arrival of the contact region terminates the observing time and then to arrange that the oncoming driver rarefaction wave arrives no sooner. This is done by appropriate selection of the length of the driver section. Thus the test time at A, located at X_A, is given by

$$\Delta t = \frac{X_A}{u_2} - \frac{X_A}{U_s} = X_A \frac{U_s - u_2}{U_s u_2} \qquad [7]$$

or, a specified test time Δt, is obtained at a distance

$$X_A = \frac{U_s u_2 \Delta t}{U_s - u_2} \qquad [8]$$

or $$X_A = a_1 M_1 \Delta t (r - 1) \qquad [9a]$$

where $r = \rho_2/\rho_1$. Here the test time Δt is in that observed in the laboratory frame. In terms of the test time, Δt_p, in the particle fr the location is

$$X_A = a_1 M_1 \Delta t_p \frac{(r - 1)}{r} \qquad [9b]$$

The time taken for the head of the rarefaction wave to reach a position X is

$$t = t_1 + \frac{X - X_1}{u_3 + a_3} \qquad [10]$$

where (X_1, t_1) comes from [5,6]. The requirement that the rarefaction wave reach X_A no earlier than the contact surface is met by setting $X = X_A$. The time for this is just X/u_2, so solving for t_2, using [6] and the fact that $u_3 = u_2$, gives

$$t_2 = \frac{X_A}{2 u_2} \qquad [11]$$

thence from [5]

$$L_{dr} = \frac{X_A a_4}{2 u_2} \left[\frac{a_4 (\gamma_4 + 1)}{2 a_4 - (\gamma_4 - 1)(u_2 - a_3)} \right]^{2(\gamma_4 - 1)/(\gamma_4 + 1)} \qquad [12]$$

Applying the adiabatic and perfect gas laws to regions 4 and 3, noting that $P_3 = P_2$, it follows that

$$a_3 = a_4 \left(\frac{P_2}{P_4} \right)^{(\gamma-1)/\gamma} \qquad [14]$$

Equation [12] now gives the minimum length for the driver section such that the head of the returning rarefaction wave arrives at the observation station, located at X_A, at the same time as the contact surface, or start of the contact region.

Reflected Shock Waves

For observations behind the reflected shock, the test time commences with the passage of this shock wave, travelling back down the shock tube (Figure A1-2 station B). This reflected shock meets the contact region and also the oncoming rarefaction wave. Reflected and transmitted waves occur. It is possible to select operating conditions so that the reflected shock wave is not reflected at the contact "surface", and thus to increase the test time, but such tailoring is not considered here and it is assumed that following this encounter some disturbance is propagated back towards the observation station at sonic speed.

If the length of the shock tube working section is L_w the reflected shock meets the contact "surface" at (X_3, t_3),

$$t_3 = \frac{L_w}{U_s} + \frac{L_w - X_3}{U_r} \qquad [15]$$

also $t_3 = X_3/u_2$, so that

$$t = \frac{L_w (U_s + U_r)}{U_s (u_2 + U_r)} \qquad [16]$$

Now the test time at station B, Figure A1-2, situated at a distance "d" from the end wall, is

$$t = t_3 + \frac{L_w - X_3 - d}{a_5} - \frac{L_w}{U_s} - \frac{d}{U_r} \qquad [17]$$

Substituting from [15] and re-arranging gives the required length of the shock tube, L_w, for a specified observation time Δt,

$$L_w = U_s \cdot \frac{U_r + u_2}{U_s - u_2} \left[\frac{a_5 \Delta t}{U_r + a_5} + \frac{d}{U_r} \right] \qquad [18]$$

The required driver length is found in the same manner as for incident shock wave observations, substituting X_3 for X_A in [12]. For observations behind reflected shock waves the test time is the same in particle and laboratory reference frames.

Results

The positions X_A, X_B, X_3 and lengths L_w and L_{dr} were calculated

using the foregoing equations. For the reflected shock waves it was assumed that the observing station was 10 cm from the end wall, so that $X_B = L_w - 10$. All lengths shown below are in cm.

M_1	Buffer	Driver	X_A	X_3	X_B	L_w	L_{dr}
incident:							
2.0	argon	helium	79				108
3.0			128				114
2.6	air	nitrogen	128				40
		helium	128				114
3.8		helium	204				125
reflected:							
1.4	argon	nitrogen		65	102	112	69
		helium		65	102	112	205
2.2		nitrogen		240	291	301	107
		helium		240	291	301	312
1.8	air	nitrogen		195	235	245	101
		helium		195	235	245	305
2.8		nitrogen		554	602	612	160
		helium		554	602	612	455

---

5. HEATED SHOCK TUBE

Introducing the active sample into the buffer gas is often a problem with compounds of low volatility. One of the options in these cases is to heat the shock tube. This heating need only apply to the working section but the coldest location will determine the vapour pressure of sample, so that the diaphragm region must also be heated. Heating can be accomplished with heating tapes and insulation, or by placing the whole shock tube in an oven. There are many difficulties in either case and the exercise is to be avoided if possible. However, it is an option to keep in mind and a temperature increase of 100 C may be considered.

Table 1 shows that the effect on required Mach number range is small, being confined chiefly to the lower range, where slightly lower Mach numbers can be used. The reduction in required shock Mach number is negligible at the top end of the temperature range.

The most important effect of raising the temperature will occur if the driver gas is heated, for then the driver section will have to be lengthened to accomodate the increased sound speed in that gas without a decrease in test time.

6. CONCLUSIONS

From the data on page A.1-5 it is clear that observations behind incident shock waves require prohibitively high driver pressures. Th estimates for reflected shock waves are reasonable for a helium drive and also possible for nitrogen drivers, especially with an argon buffer. Considering the required test time of 0.002 second the positions of observing stations may be computed for both incident and reflected shocks: the results are given on page A.1-13. These show t with a helium driver gas the driver would have to about 5 metres long in order to avoid premature truncation of the test time. This length is excessively extravagant with an expensive gas so it is recommended that a nitrogen driver be used, preferably with an argon buffer. Thi combination requires a shock tube with a working section of length 3 metres and a 1 metre driver section. The shock wave is not formed immediately upon diaphragm rupture but reaches peak strength some distance downstream, before decaying through boundary layer action. This formation distance may be about 30 shock tube diameters so that peak strength is reached at about 2 metres for a shock tube diameter of 6.5 cm. The pressures are quite high so the tube bore may be 2-inches or less, as convenient.

Boundary layer growth has not been considered in this study but is not expected to be a limiting factor or to interfere with the measurements. An aspect which does require further thought is that o sample introduction. The simplest way for materials of low volatilit is to suspend a drop, or some coated substrate such as mylar, for the shock wave to heat as it passes. With observations behind the

reflected shock wave sample introduction must be sufficiently far upstream of the observing station that it does not act as a heat sink to the sample being studied. It may be desirable to study a uniform medium by pre-dispersing the sample in the buffer gas. If this requirement means a heated shock tube then some further design though is needed. It would probably be best if the shock tube were completely contained within an oven, possibly using a fairly small bore tube, and the possibilities of a shock wave valve, in place of the diaphragm, should also be considered. This valve has the attraction that a succession of shocks could be fired without opening the oven, but the expansion characteristics are different and would have to be considered further.

References

Bradley J.N.
Shock Waves in Chemistry and Physics
Methuen & Co. Ltd., London, 1962.

Cann M.W.P.
Fundamentals of Shock Tube Design
Rolls Royce Ltd., internal report 15th June 1959

Courant R., Friedrichs K.O.
Supersonic Flow and Shock Waves
Interscience Pubs. Inc., New York, 1948

Glass I.I., Hall J.G.
Handbook of Supersonic Aerodynamics. Section 18. Shock Tubes
NAVORD Report 1488 (Vol 6), December 1959

Gordon S., McBride B.J.
Computer Program for Calculation of Complex Chemical Equilibrium Compositions, Rocket Performance, Incident and Reflected Shocks, and Chapman-Jouguet Detonations.
NASA Lewis Research Center, NASA SP-273, 1971.

Muirhead J.C., Jones W.A.
Shock wave valves
Rev.Sci.Instr.,35(1),119-120 (1964)
Also reports of the Suffield Experimental Station, Alberta.

Resler E.L., Lin S.-C., Kantrowitz A.
The production of high temperature gases in shock tubes.
J.Appl.Phys.,23(12),1390-1399 (1952).

Seeker W.R., Lester T.W., Merklin J.F.
Shock tube techniques in the study of pulverized coal ignition ar burnout.
Rev.Sci.Instr.,51(11),1523-1531 (1980).

Watson R., Morsell A.L., Hooker W.J.
Techniques for conducting shock tube experiments with mixtures of ultrafine solid particles and gases.
Rev.Sci.Instr.,38(8),1052-1057 (1967).

Wright J.K.
Shock Tubes
Methuen & Co. Ltd., London, 1961.

TABLE 1. Shock Wave Conditions

	Monatomic Gas (γ_1=5/3)			Diatomic Gas (γ_1=7/5)		
M_1	P_2/P_1	ρ_2/ρ_1	T_2/T_1	P_2/P_1	ρ_2/ρ_1	T_2/T_1
1.2	1.550	1.297	1.195	1.513	1.342	1.128
1.4	2.200	1.581	1.392	2.120	1.690	1.255
1.6	2.950	1.842	1.602	2.820	2.032	1.388
1.8	3.800	2.077	1.830	3.613	2.359	1.531
2.0	4.750	2.286	2.078	4.500	2.667	1.688
2.2	5.800	2.469	2.349	5.480	2.951	1.857
2.4	6.950	2.630	2.643	6.553	3.212	2.040
2.6	8.200	2.770	2.960	7.720	3.449	2.238
2.8	9.550	2.893	3.301	8.980	3.664	2.451
3.0	11.000	3.000	3.667	10.333	3.857	2.679
3.2	12.550	3.094	3.229	11.780	4.031	2.922
3.4	14.200	3.176	4.471	13.320	4.188	3.180
3.6	15.950	3.248	4.911	14.953	4.330	3.454
3.8	17.800	3.312	5.375	16.680	4.457	3.743
4.0	19.750	3.368	5.864	18.500	4.571	4.047

TABLE 2. Driver Pressure Ratios

Driver:	Argon	Nitrogen		Helium	
γ_4 :	5/3	7/5		5/3	
Buffer:	Argon	Argon	Air	Argon	Air
γ_1 :	5/3	5/3	7/5	5/3	7/5
a_4/a_1:	1.000	1.094	1.015	3.162	2.933
M_1		P_4/P_1			
1.2	2.507+0	2.224+0	2.337+0	1.796+0	1.806+0
1.4	5.633+0	4.391+0	4.892+0	2.907+0	2.996+0
1.6	1.193+1	8.055+0	9.564+0	4.406+0	4.578+0
1.8	2.449+1	1.408+1	1.790+1	6.378+0	6.764+0
2.0	4.981+1	2.380+1	3.257+1	8.929+0	9.681+0
2.2	1.020+2	3.936+1	5.827+1	1.219+1	1.353+1
2.4	2.134+2	6.409+1	1.034+2	1.631+1	1.855+1
2.6	4.639+2	1.034+2	1.829+2	2.148+1	2.506+1
2.8	1.068+3	1.425+2	3.250+2	2.792+1	3.347+1
3.0	2.673+3	2.056+2	5.826+2	3.594+1	4.430+1
3.2	7.541+3	4.295+2	1.059+3	4.585+1	5.820+1
3.4	2.544+4	6.904+2	1.964+3	5.809+1	7.603+1
3.6	1.142+5	1.124+3	3.733+3	7.318+1	9.889+1
3.8	8.552+5	1.851+3	7.326+3	9.175+1	1.282+2
4.0	2.071+7	3.091+3	1.496+4	1.146+2	1.659+2

TABLE 3. Conditions Behind Reflected Shock Waves

	Monatomic Gas (γ_1=5/3)			Diatomic Gas (γ_1=7/5)		
M_1	P_5/P_1	T_5		P_5/P_1	T_5	
		T_1=296K	T_1=373K		T_1=296K	T_1=373K
1.1	1.576	355 K	448 K	1.540	335 K	422 K
1.2	2.317	416	525	2.238	374	470
1.4	4.330	545	687	4.168	453	568
1.6	4.089	687	866	6.897	537	671
1.8	10.621	844	1064	10.495	627	780
2.0	14.929	1018	1282	15.017	723	897
2.2	20.004	1207	1521	20.495	826	1020
2.4	25.833	1414	1782	26.944	934	1151
2.6	32.398	1638	2064	34.395	1048	1290
2.8	39.680	1879	2368	42.864	1169	1436
3.0	47.663	2138	2694	52.376	1295	1589
3.2	56.337	2414	3042	62.958	1428	1747
3.4	65.689	2708	3412	74.590	1565	1912
3.6	75.715	3019		87.312	1708	
3.8	86.383	3349		101.11	1855	
4.0	97.703	3695		115.99	2006	

Figure A1-1. (x,t) Shock Tube Diagram - Incident Wave Study

p	particle trajectory
t_1	rarefaction head (H) overtakes tail (T)
t_2	contact surface (CS) arrives at X_A
Δt_A	observation time at station A
D	diaphragm station
L	length of driver section
SW	incident shock wave

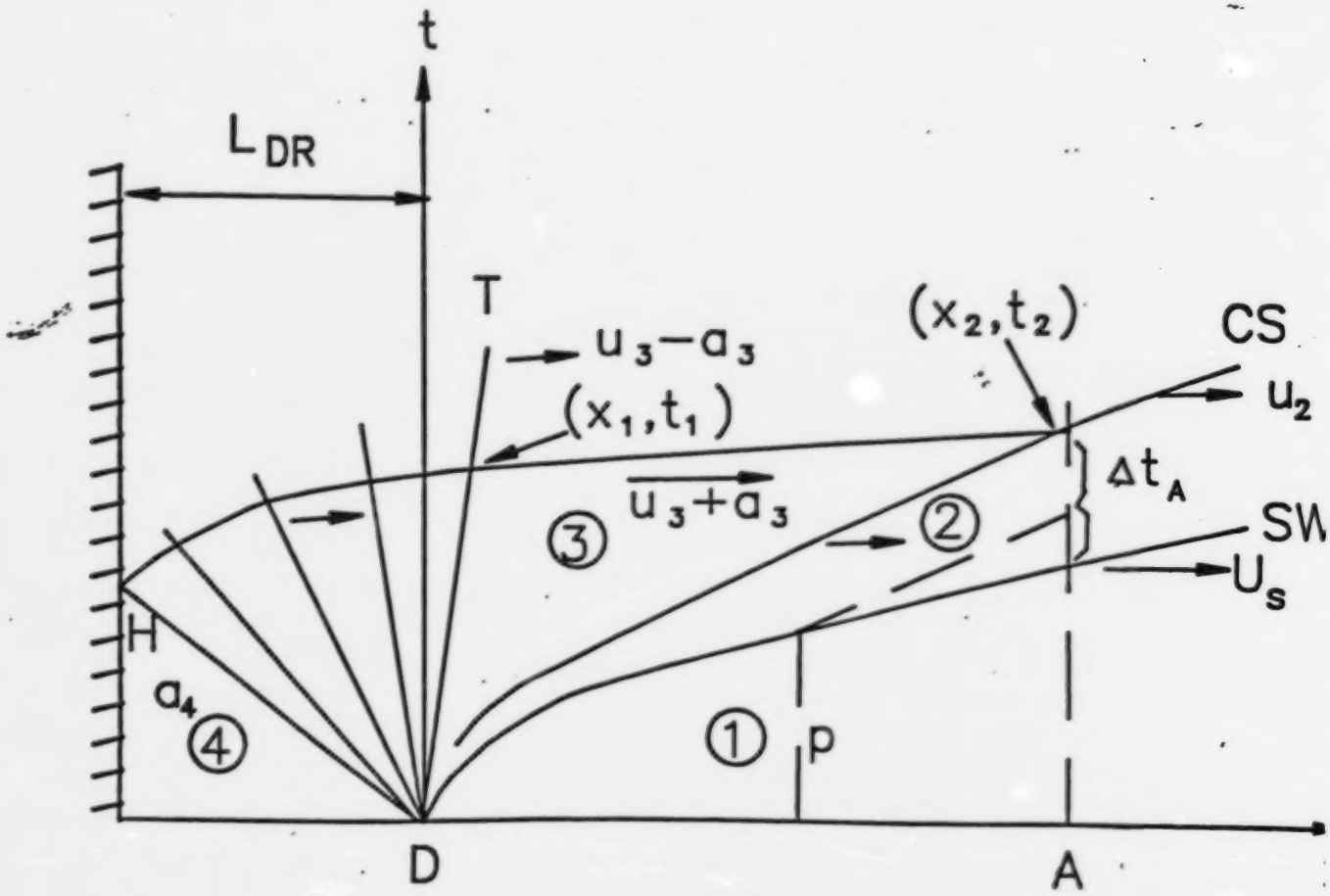

Figure A1-2. (x,t) Shock Tube Diagram - Reflected Wave Study

t_1 rarefaction head (H) overtakes tail (T)

t_2 contact surface (CS) arrives at X_A

t_3 contact surface meets reflected shock wave (RW)

Δt_B observation time at station B

D diaphragm station

L length of driver section

L length of working section

SW incident shock wave

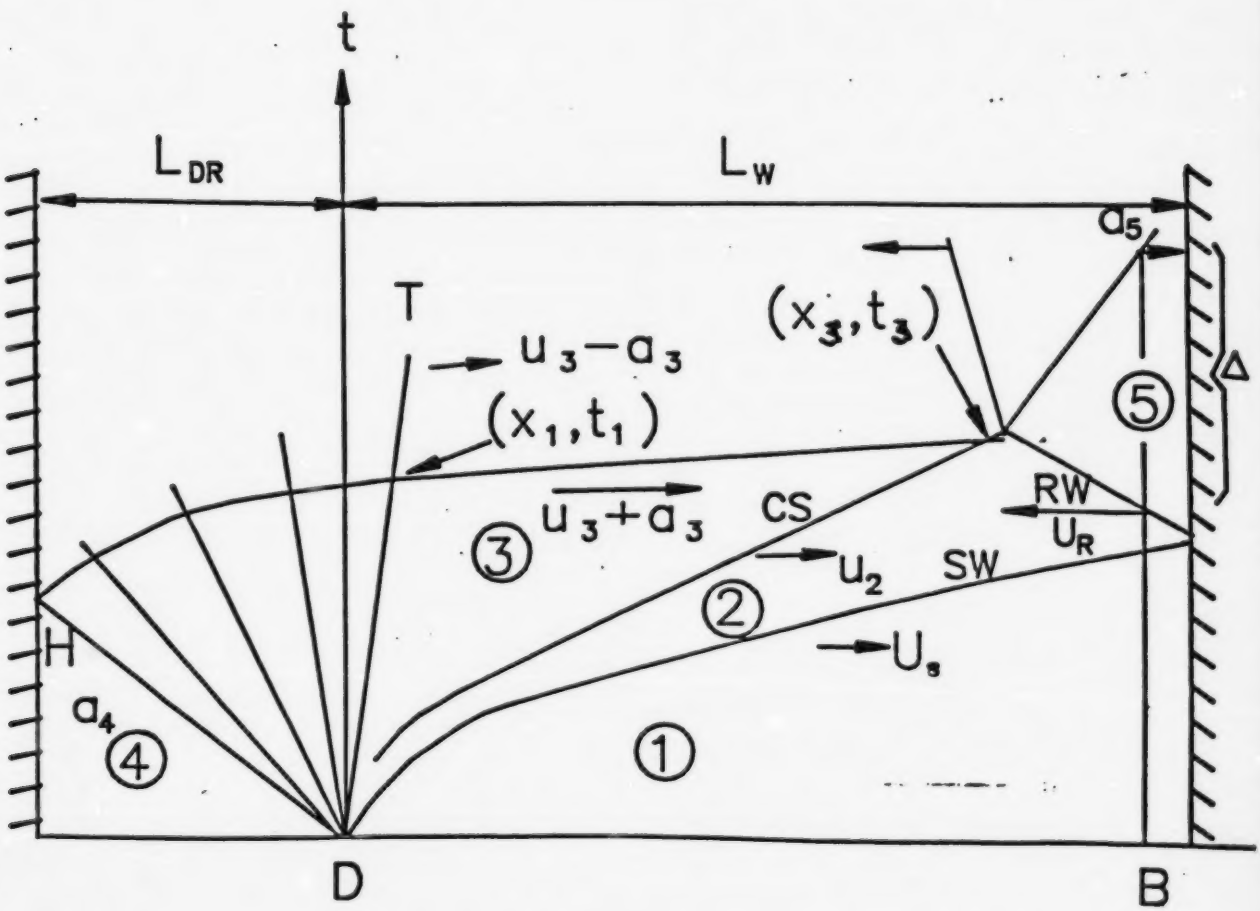

Appendix - 2. Shock Tube Diagnostics

M.W.P.Cann

		Page
1.	INTRODUCTION	2
2.	TEMPERATURE MEASUREMENT	3
	(a) Infra-Red Nitrogen Absorption and Emission	4
	(b) UV Nitrogen Absorption	5
	(c) UV Oxygen Absorption	6
3.	HYDROGEN DENSITY MEASUREMENT	7
	Absorption Spectroscopy	7
	Sampling	8
4.	LASER RAMAN METHODS	9
	Spontaneous Raman Spectroscopy	9
	Stimulated Raman Spectroscopy (SRS)	10
	Coherent Anti-Stokes Raman Spectroscopy (CARS)	11
5.	CONCLUSIONS	13
References		15

1. INTRODUCTION

An attractive feature of the shock tube is its simplicity and the way in which the thermodynamic state behind the shock wave can be deduced from a knowledge of the pre-shocked conditions and the shock speed. Quite often the values for pressure and temperature deduced in this manner are sufficiently accurate. Sometimes this is not the case, however, especially when chemical reactions are taking place, or perhaps behind the reflected shock wave, since the calculation error increases with successive shocks. It is assumed here that the temperature has to be measured.

Measurement of shock speed has been routine for some thirty years and presents no difficulties. For the low shock Mach numbers encountered here there is no siginificant ionisation of the gas, so thin-film platinum resistance gauges can be used. These devices are simple to make and use and have a response time of about 1 μsec, or the transit time of the shock wave across the film, whichever is the greater. A sharp voltage pulse is generated which is suitable for triggering counters and other equipment.

Pressure measurement, similarly, is a standard procedure. Piezo-electric transducers of the type manufactured by the Kistler Corp. have high sensitivity and a rapid response, with a slightly slower rise-time than that of the thin-film gauges. These are well tried and reliable devices.

The studies to be conducted concern the de-hydrogenation and combustion onset of various aromatic hydrocarbons. Combustion onset

is monitored easily enough by recording the time history of the light emitted by the shock heated sample. Using a photomultiplier in the visible part of the spectrum one may be selective and observe particular radicals. Similar observations may be made in the infrared. Of much greater difficulty is the measurement of free hydrogen density, and it this problem which is addressed here.

The most attractive methods in shock tube diagnostics, and usually the best, are optical or spectroscopic. These are non-invasive, usually very fast and capable of delivering time histories following shock heating. A fundamental problem in the present situation is the fact that none of argon, nitrogen or hydrogen absorb in the visible, near ultra-violet or infra-red, except for weak pressure-induced absorption by nitrogen, and weak quadrupole transitions in hydrogen. Vibrational-rotational transitions are forbidden in the absorption of spectra of homonuclear molecules, such as N_2 and H_2, but not in their Raman spectra. This fact has been used by a number of workers for diagnostic purposes and appears to offer a favourable solution here. Other methods are also discussed.

2. TEMPERATURE MEASUREMENT

The only practical methods for temperature measurement are spectroscopic and these are based on sensing the Boltzmann population distribution amongst its states of some suitable marker molecule or atom. As such it is expedient to select a stable, uniformly

distributed species, such as the buffer gas. Temperatures derived from measurements on the hydrocarbon molecules are unlikely to be accurate, but might be used to yield the relevant local value under non-uniform conditions. Since the first excited state in argon lies at 93144 cm^{-1} (1) there is no Boltzmann distribution to interrogate and it cannot be used. In this case a seed gas must be introduced, possibly 10% of nitrogen, which would not affect the shock wave properties significantly.

In some experimental situations temperatures have been measured by stimulating a gas into fluorescence and measuring the profile of line strengths in the resulting rotational spectrum. Such a procedure can be adapted to vacuum UV absorption through laser frequency doubling techniques (2,3). However, with pressures of 20 atmospheres the mean free time between collisions is 10^{-10} sec or less, appreciably shorte than radiative lifetimes, so the radiation will be quenched. There remains, then, absorption or emission spectroscopy and laser Raman spectroscopy. This last appears to be the best prospect and is considered separately later on.

(a) Infra-Red Nitrogen Absorption and Emission

Infrared absorption occurs between 2100 and 2600 cm^{-1} (4) but the absorption coefficient is low. For a pressure of 20 atmospheres of nitrogen the absorption coefficients for temperatures of 400 and 800 K are, very approximately, 0.0004 and 0.0001 cm^{-1} respectively. This level of absorption could only be used with about 350 traversals of a 10 cm shock tube path. In emission the path radiance is 3 μ-watts/(ster.cm^2) at 400 K and 7 μ-watts at 800 K, compared with a background of 40 μ-watts, so this is unusable.

(a) UV Nitrogen Absorption

Absorption from the ground state of nitrogen occurs only in the vacuum ultraviolet (5). The Vegard-Kaplan bands at 180 nm are too weak to be useful. Further into the UV, Appleton and Steinberg (6,7) have measured the absorption of shock-heated nitrogen in the region 108.6 to 133.4 nm, where absorption ocurs in the Lyman-Birge-Hopfield ($a^1\Pi_g \leftarrow X^1\Sigma^+_g$) and Tanaka ($c^3\Pi_u \leftarrow X^1\Sigma^+_g$, $w^1\Delta_u \leftarrow X^1\Sigma^+_g$) band systems. The best known of these, which also absorbs at the longest wavelengths, is the first, and it is considered here for temperature measurement.

From the the pertinent constants (8) the positions of these bands can be calculated. These are shown below along with integrated band absorption coefficients, which were obtained by applying the Franck-Condon factors of McCallum, Jarmain and Nicholls (9) to the measurements of Ching, Cook and Becker (10) - the value for the (3,0) band was used as a reference.

v' ,v''	ν_0	Band Int.Abs.
0,0	145.0 nm	25
1,0	141.6	69
2,0	138.3	103
3,0	135.3	112
4,0	132.4	98
5,0	129.7	75
0,1	150.1	91
1,1	146.4	118
2,1	143.0	61
3,1	139.7	8
4,1	136.7	3
5,1	133.8	27

Assuming a Gaussian shape for each band, with a half-width of 200 cm^{-1} (FWHM), judged from the paper by Ching et al., gives the peak band absorption coefficient as 0.1475 of the band integrated absorption. From this, for a 10 cm optical path through the shock tube, the density of nitrogen required to give a peak absorption of 67% can be calculated. The results, expressed as a percentage of the 20 atmosphere pressure in the shock tube, are as follows,

Band	Temperature	$[N_2]$
0,0	400 K	0.015 %
	800	0.054
0,1	400	1300.
	800	8.33

Concentrations for the (0,0) band demonstrate the strong absorption of these bands, where only trace quantities of N_2 suffice. On the other hand the population of the v"=1 vibrationa level in the ground state is inadequate for using this progressio at 400 K. It is immediately obvious that it is not possible to measure temperature by monitoring the ratio of populations in two vibrational levels, so that this would have to be done by measuring the absorption at two or more positions in the rotational spectrum of the same band. There are two reasons why this is unlikely to be sucessful. First, the bands are quite compact (11), so a spectral resolution of about 0.1 nm would be required. More importantly the measurements would have to be mad in the v"=1 progression, but this overlaps the very much stronger v"=0 bands, which would therefore vitiate the measurements. Thus this band system can only be used for the measurement of temperature where trace quantities of N_2 can be introduced, i.e. not in air.

(a) UV Oxygen Absorption

Oxygen absorbs in the near and vacuum UV through the strong Schumann-Runge ($B^3\Sigma_u^- \leftarrow X^3\Sigma_g^-$) and Herzberg ($A^3\Sigma_u^+ \leftarrow X^3\Sigma_g^-$, $c^1\Sigma_u^- \leftarrow X^3\Sigma_g^-$, $A'^3\Delta_u \leftarrow X^3\Sigma_g^-$) continuum and band systems. Many measurements have been made on these absorption systems which are therefore well described quantitatively. A series of calculation on the absorption by oxygen has been published (12) and can be used to assess the suitability for temperature measurement. The calculation steps were 300, 600, 1000,...K and 1, 10, 25 and 50 atmospheres pressure. These are close enough to the experimental conditions being investigated. The significance here of the tota pressure of 20 atmospheres is in the broadening of the spectral lines. In the following calculations it is assumed that the working medium is air, thus fixing the concentration of O_2.

Pursuing reasoning similar to that used with the UV absorption of N_2, one requires absorption in the range 20 to 80 %, for a 10 cm path in 20 atmospheres of air, at 400 and 800 K. Adjusting these requirements to absorption coefficients at STP it is found that they can be met as follows,

	Abs. Coeff.		Wavelengths		
400 K	0.0080 to 0.060		235.0 to 275.0		nm
800	0.016	0.010	200.0	225.0	

The problem here lies in the extensive nature of the Schumann-Runge band system whith has very many overlapping bands. As the temperature rises these bands develope rapidly and spread, as can

be seen in the paper by Cann et al (12). Thus it is not possible to obtain the temperature through measurements on bands originating on two different vibrational levels. Measured intensities would have to be subjected to a detailed line-by-line analysis, for which pre-calculated tables might be used. The feasibility and precision of temperature measurements made this way cannot be assessed without making similar detailed calculations.

3. HYDROGEN DENSITY MEASUREMENT

The information required is actually the number of moles of hydrogen produced per initial mole of hydrocarbon molecule, rather than the actual number density of hydrogen. This means that post shock assay may be used, as well as optical methods. Several techniques are discussed here and, separately, the laser Raman methods.

Absorption Spectroscopy

Excepting very weak transitions in the far infrared, molecular hydrogen absorbs only in the vacuum ultraviolet, where the most accessible band systems are the Lyman and Werner bands. Patch (13) measured the dissociation rate of hydrogen by monitoring the (0,3) band of the Werner system, centered at 114.8 nm, in shock heated argon containing from 1 to 30% of H_2. His measurements were conducted at temperatures in excess of 2000 K so that higher vibrational levels

were populated significantly, but in the present circumstances the (0,3) band cannot be used. Unlike the temperature measurement it is necessary to monitor absorption at only one wavelength. Also hydrogen densities are much lower and the strong UV absorption bands are more likely to be useful. A very likely problem is absorption by the much more abundant hydrocarbon material and in view of this uncertainty the technique must be placed low on the list of choices. While this method is not ruled out entirely, other methods appear to be more attractive.

Sampling

After the shock tube has been fired a sample of the resultant gas is withdrawn for chemical assay. This procedure has been used, for example, by Tsang (14), Tschuikow-Roux and Marte (15), Vaughn et al (16). The last two papers describe the use of an in-line ball valve, of the Jameson type, by means of which the end section of the shock tube is isolated immediately after the shock tube has been fired. There is always the problem of turbulent mixing up and down the tube, mixing with the driver gas and possible contamination with wall material. If the hydrocarbon sample is introduced in a non-uniform manner then the results may also be degraded by the presence of hydrocarbon which failed to volatilise completely.

An improvement on the above method, albeit a much more complex operation, is the prompt analysis of the shock-heated sample by time-

of-flight mass spectrometry (17,18,19,20,21). Here the shock tube is the source for a molecular beam which is generated by expanding the gases from behind the reflected shock wave. The rarefied and accelerated gas passes through a series of skimmers to produce a collimated beam for analysis. This is an experimentally difficult technique which would incur a lengthy development time.

4. LASER RAMAN METHODS

Reviews of laser Raman spectroscopy have been given by Demtroder (2) and by Lederman (22). Raman spectroscopy is particularly appropriate for diagnoses in nitrogen and hydrogen gases, where selection rules of absorption spectroscopy preclude infrared monitoring. With the high intensity of the laser it is feasible to monitor gases at low concentrations. Three different applications of the Raman effect which are in current use are described and discussed.

Spontaneous Raman Spectroscopy

The incident radiation (laser beam) raises a molecule into an excited state, real or virtual, from which it decays. The final state may be the same as the initial, Rayleigh scattering, a higher state, giving rise to Stokes lines, or a lower state if the initial state is already an excited one, giving anti-Stokes lines. Anti-Stokes lines

are weaker than Stokes because the population of the initial states is a thermally governed Boltzmann distribution. The Stokes and anti-Stokes lines usually arise from different vibrational energy levels and so are bands, with accompanying rotational structure, but pure rotational spectra are also observed on either side of the laser line.

This basic Raman scattering process produces very weak spectra and, furthermore, is confounded by extraneous fluorescence from the gas, windows and walls and is unlikely to be successful in shock tube studies. The two methods which follow avoid the fluoresence problem and offer intensities greater by factors of 10^4 to 10^5.

Stimulated Raman Scattering (SRS)

With very intense incident beams, and consequently strong Raman scattering, the molecules interact with both the laser frequency and the Stokes frequency, the two waves being coupled by the molecular transition. In this situation there may be an energy exchange between the laser pump frequency and the Stokes and anti-Stokes lines, resulting in strong directional output of the Raman lines, which may have intensities comparable with the pump frequency. Also, with this technique the emitted anti-Stokes radiation, which is not necessarily much weaker than the Stokes radiation, is subject to phase matching and emerges in a cone with axis parallel to the incident laser beam. The application of SRS is discussed by Owyoung (23) who considers variations, including two-beam non-linear interferometry and

heterodyning.

In this method a linearly polarised pump beam is modulated and passed, with a probe beam at a second frequency, through the medium being investigated. The intensity modulation of the emergent beam is then proportional to the density of the Raman active molecule. This method has been applied to measurements on hydrogen (24,25,26,27) but not, apparently, in the shock tube. Use of the technique is limited by the high threshold intensities required for the pump beam (2).

Coherent Anti-Stokes Raman Spectroscopy (CARS)

CARS has received considerable attention and has been used in several diagnostic situations, including flames and shock tubes (22,26,28). The technique requires two laser beams at different frequencies, ω_1 and ω_2, whose difference equals the frequency of the Raman active transition, ω_v. For example, if the Raman transition is between the two lowest vibrational levels then $h\omega_v$ is the energy separating them. The pump frequency, ω_1, populates the virtual level from which Stokes emission is stimulated by ω_2, bringing the molecule to the upper level in the Raman transition. From here it is stimulated by ω_1 to another virtual state from which it decays emitting the anti-Stokes line at a frequency of $\omega_1+\omega_v$. Although the description has been given in terms of absorption and emission, in fact this is a four-wave mixing process and the anti-Stokes line is emitted instantaneously. The technique requires phase matching

between ω_1 and ω_2 but at optical frequencies this is achieved satisfactorily with collinear beams.

In practice the same laser is used to generate ω_1 and to pump a tunable dye laser which generates ω_2. But, more elegantly, some situations permit using SRS to generate the appropriate Stokes line for ω_2 in a high pressure cell containing the gas to be probed: this is usually done with measurements on hydrogen.

The CARS method offers much higher signal intensities than spontaneous Raman spectroscopy, small beam divergence and high spectral resolution. Since it is the anti-Stokes line that is detected this allows filtering out all lower frequencies, and hence all fluorescence induced by the laser lines. Disadvantages are the non-linear dependence on molecular density and sensitivity to beam instabilities. Nevertheless it has been successfully used in many experimental situations.

The measurment of temperature in a shock tube by CARS is described by Knapp and Hindelang (29) by probing N_2. A frequency doubled, Q-switched Nd-Yag laser and a pulsed dye laser were used. The Raman transition was selected to be a particular rotational line in the (1,0) vibrational band. The shock conditions were repeated with different rotational lines to build up the rotational spectrum, from which the temperature was obtained. The method was successfully used for temperatures in the range 700 to 2400 K. An obvious disadvantage is the failure to obtain the temperature for each individual shock.

Measurement of hydrogen density has been made in flames by Moya, Regnier et al (28,31) and in a shock tube by Matsumoto (25), and also by Lederman et al (26). In these cases radiation at the pump frequency, ω_1, was generated by a Q-switched ruby laser and part of this radiation was passed through a cell containing H_2 to obtain ω_2 by SRS. Regnier et al measured H_2 densities in the range 10 to 106 ppm and expected to improve the lower concentration limit by a factor 2 to 3.

5. CONCLUSIONS

The foregoing discussion has considered a variety of techniques for temperature and density measurement behind shock waves. The most promising method, which is applicable to both requirements, is the CARS method in laser Raman spectroscopy. This method has already been applied successfully to temperature measurement in a shock tube, probing N_2 as may be done here. It has also been used to measure H_2 densities, both in a shock tube and in flames. These facts bode well for the application of CARS to the studies under discussion in this report. Furthermore a recent paper (32) discusses the simultaneous monitoring of more than one species and some such scheme may be utilised to perform both temperature and density measurements at the same time.

Of the more conventional methods considered it is clear that

absorption spectroscopy would have to be conducted in the vacuum ultraviolet. Nitrogen cannot be used for temperature measurement except as a trace species in an argon buffer, when the concentration must be adjusted for the temperature regime. High spectral resolution is required in order to probe the rotational structure of a single band, since the temperature cannot be obtained from relative band strengths. Hydrogen density measurements might be made in a similar way. They would be simpler in that radiation needs to be monitored at only one wavelength. However, it is anticipated that the presence of larger quantities of hydrocarbon molecules would successfully obstruct the measurement. While the use of "in-line" mass spectrometry would be regarded as a last resort, post shock sampling can be considered, even as a back-up or for comparison with diagnosis by CARS.

References

1. Moore C.E.
Atomic Energy Levels, Vol I.
NBS Circular 467, 15th June 1969

2. Demtroder W.
Laser Spectroscopy
Springer-Verlag, New York, 1981

3. Filseth S.V., Wallenstein R., Zacharias H. Two photon excitation of CO ($A^1\Pi$) and N_2 ($a^1\Pi$)
Opt.Comm.,23,231-235 (1977)

4. Reddy S.P., Cho C.W.
Induced infrared absorption of nitrogen and nitrogen-foreign gas mixtures
Can.J.Phys.,43,2331-2343 (1965)

5. Herzberg G.
Molecular Spectra and Molecular Structure. I. Diatomic Molecules
D. van Nostrand Inc., Princeton, 1950.

6. Appleton J.P., Steinberg M.
The vacuum ultraviolet absorption of shock-heated vibrationally excited nitrogen
General Motors Corp., ARPA Order No. 347, Project Code No. 7400, July 1966

7. Appleton J.P., Steinberg M.
Vacuum ultraviolet absorption of shock heated vibrationally excited nitrogen
J.Chem.Phys.,46(4),1521 (1967)

8. Herzberg G., Huber K.P.
Molecular Spectra and Molecular Structure. IV. Constants for Diatomic Molecules
Van Nostrand Reinhold Co., New York (979)

9. McCallum J.C., Jarmain W.R., Nicholls R.W.
Franck-Condon factors and related quantities. II. Additional diatomic molecular band systems of N_2
York University, CRESS Spectroscopic Report No. 3, March 1972

10. Ching B.K., Cook G.R., Becker R.A.
Oscillator strengths of the a, w and C bands of N_2
J.Quant.Spectrosc.Radiat.Transf.,7(2),323-330 (1967)

11. Vanderslice J.T., Tilford S.G., Wilkinson P.G.
The high resolution absorption spectrum of nitrogen from 1060 to 1520 A. I. The $a^1\Pi g \rightarrow X^1\Sigma g$ system
Ap.J.,141(2),395-426 (1965)

12. Cann M.W.P., Shin J.B., Nicholls R.W.
Oxygen absorption in the spectral range 180-300 nm for temperatures to 3000 K and pressures to 50 atm
Can.J.Phys.,62(12),1738-1751 (1984)

13. Patch R.W.
Shock-tube measurement of dissociation rates of hydrogen
J.Chem.Phys.,36(7),1919-1924 (1962)

14. Tsang W.
Thermal decompositon of some tert-butyl compounds at elevated temperatures
J.Chem.Phys.,40(6),1498-1505 (1964)

15. Tschuikow-Roux E., Marte J.E.
Thermal decomposition of fluoroform in a single-pulse shock tube. I.
J.Chem.Phys.42(6),2049-2056 (1965)

16. Vaughn S.N., Lester T.W., Merklin J.F.
A single pulse shock tube study of soot formation from benzene pyrolysis
Shock Tubes and Waves, Proceedings of the 13th Intl. Symp., Ed. C.E. Treanor, J.G. Hall
State University of New York Press, Albany, 1981, page 860.

17. Bradley J.N., Kistiakowsky G.B.
Shock wave studies by mass spectrometry
J.Chem.Phys.,35(1),256-263 (1961)

18. Gutman D., Hay A.J., Belford Shock wave studies with a quadrupole mass filter. I. Experimental apparatus: its design and performance
J.Phys.Chem.,70(6),1786-1792 (1966)

19. Krizancic I., Haluk M., Cho S.H., Trass O.
Shock tube coupled to the time-of-flight mass specgrometer as a molecular beam sampling system
Rev.Sci.Instr.,50(7),909-915 (1979)

20. Teshima K., Takahashi N., Deguchi M.
An application of the molecular beam time-of-flight technique to measuremen ts of thermal boundary layer effects on mass sampling from a shock tube
Shock Tubes and Waves, Proceedings of the 13th Intl. Symp., Ed. C.E. Treanor, J.G. Hall
State University of New York Press, Albany, 1981, page 116.

21. Gray I.D., Kern R.D., Kistiakowsky G.B., Niki H.
Pyrolysis of ethylene in shock waves
J.Chem.Phys.,45(7),2371-2377 (1966)

22. Lederman S.
Developments in laser based diagnostic techniques
Shock Tubes and Waves, Proceedings of the 12th Intl. Symp.,
Ed. A. Lifshitz, J. Rom
The Magnes Press, The Hebrew University, Jerusalem 1980, p 48.

23. Owyoung A.
Coherent Raman gain spectroscopy using CW laser sources
IEEE J.Quant.Electron.,QE-14(3),192-203 (1973)

24. Lee S.A., Wallenstein R., Hansch T.W.
Hydrogen 1S-2S isotope shift and 1S Lamb shift measurements by laser spectroscopy
Phys.Rev.Lett.,35(19),1262-1266 (1975)

25. Matsumoto Y., Matsui H., Asaba T. Rotational relaxation of H_2 in nozzle flow
Shock Tubes and Waves, Proceedings of the 13th Intl. Symp., Ed.
C.E. Treanor, J.G. Hall
State University of New York Press, Albany, 1981, page 553.

26. Lederman S., Celentano A., Glaser J.
Temperature, concentration and velocity in jets, flames and shock tubes.
Phys.Fluids,22(6),1065-1072 (1979)

27. Lallemond P., Simova P., Bret G.
Pressure-induced line shift and collisional narrowing in hydrogen gas determined by stimulated Raman emission
Phys.Rev.Lett.,17(25),239-1241 (1966)

28. Regnier P.R., Taran J.P.E.
On the possibility of measuring gas concentrations by stimulated anti-Stokes scattering
Appl.Phys.Lett.,23(5),240-242 (1973)

29. Knapp K., Hindelang F.J.
Measurement of temperatures in a shock tube by coherent anti-Stokes Raman spectroscopy (CARS)
Shock Tubes and Waves, Proceedings of the 13th Intl. Symp., Ed.
C.E. Treanor, J.G. Hall
State University of New York Press, Albany, 1981, page 132.

30. Regnier P.R., Moya F., Taran J.P.E.
Gas concentration measurement by coherent Raman anti-Stokes scattering
AIAA J.,12(6),826-831 (1974)

31. Moya F., Druet S.A.J., Taran J.-P.E.
Rotation-vibration spectroscopy of gases by coherent anti-Stokes Raman scattering: application to concentration and temperature measurements
Lecture Notes in Physics 43. Laser Spectroscopy,
Ed by S.Haroche, J.C.Pebay-Peyroula, T.W.Hansch, S.E.Harris
Proceedings of the 2nd Intnatl. Conf., Megere, June 1975
Springer-Verlag, New York (1975).

32. Eckbreth A.C., Anderson T.J.
Dual broadband CARS for simultaneous, multiple species measurements
Appl.Opt.,24(16),2731-2736 (1985)